Food Chemistry 457 (2024) 140161

Contents lists available at ScienceDirect

Food Chemistry

journal homepage: www.elsevier.com/locate/foodchem

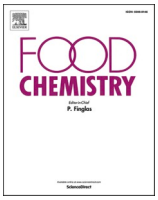

Untargeted metabolomics unravels distinct gut microbial metabolites derived from plant-based and animal-origin proteins using *in vitro* modeling

David Izquierdo-Sandoval [a], Xiang Duan [b,c], Christos Fryganas [c], Tania Portolés [a], Juan Vicente Sancho [a], Josep Rubert [c,d,*]

[a] *Enviromental and Public Health Analytical Chemistry, Research Institute for Pesticides and Water (IUPA), Universitat Jaume I, Av. Sos Baynat S/N, 12071 Castellón de la Plana, Spain*
[b] *College of Food Science and Engineering, Northwest A&F University, Yangling 712100, PR China*
[c] *Food Quality and Design, Wageningen University & Research, Bornse Weilanden 9, Wageningen 6708, WG, The Netherlands*
[d] *Division of Human Nutrition and Health, Wageningen University & Research, Stippeneng 4, Wageningen 6708, WE, The Netherlands*

ARTICLE INFO

Keywords:
Gut microbial metabolites
Protein fermentation
Plant-based proteins
Metabolomics
High-resolution mass spectrometry

ABSTRACT

The popularity of plant-based meat alternatives (PBMAs) has sparked a contentious debate about their influence on intestinal homeostasis compared to traditional animal-based meats. This study aims to explore the changes in gut microbial metabolites (GMMs) induced by the gut microbiota on different digested patties: beef meat and pea-protein PBMA. After digesting *in vitro*, untargeted metabolomics revealed 32 annotated metabolites, such as carnitine and acylcarnitines correlated with beef meat, and 45 annotated metabolites, like triterpenoids and lignans, linked to our PBMA. Secondly, (un)targeted approaches highlighted differences in GMM patterns during colonic fermentations. Our findings underscore significant differences in amino acids and their derivatives. Beef protein fermentation resulted in higher production of methyl-histidine, gamma-glutamyl amino acids, indoles, isobutyric and isovaleric acids. In contrast, PBMAs exhibit a significant release of N-acyl amino acids and unique dipeptides, like phenylalanine-arginine. This research offers valuable insights into how PBMAs and animal-based proteins differently modulate intestinal microenvironments.

1. Introduction

Plant-based meat analogs (PBMA) have emerged as a popular alternative, appealing to health- and environmentally-conscious consumers with organoleptic characteristics similar to traditional meat products. They are constituted of pure (or partially purified) plant proteins (*e.g.*, soybean, pea, grain, *etc.*), vegetable oils, binding agents, and other ingredients such as preservatives and sweeteners (De Marchi et al., 2021). Animal and plant proteins undergo digestion in the gastrointestinal (GI) tract, interacting with trillions of microorganisms in the lower intestine. Bacterial proteases hydrolyze proteins and large peptides into small peptides and single amino acids (AAs), which are fermented to produce short-chain fatty acids (SCFA), branched-chain fatty acids (BCFA), ammonia, amines, hydrogen sulfide, phenols, indoles, among other protein-derived gut microbial metabolites (GMM). Furthermore, the intestinal microbiota can also recycle nitrogen and synthesize AAs *de novo* (Portune et al., 2016). These microbial-related metabolites, either as a single agent or in combination, can affect the luminal microenvironments and intestinal epithelial cells. Furthermore, GMMs, whose production is influenced by the source of protein and other macronutrients in the food matrix, play a crucial role in the host's metabolic, immune, and neurological systems (Blachier et al., 2017).

The impact of substituting animal-derived proteins with plant-based proteins *via* PBMA on gut homeostasis remains unclear. On the one hand, excessive red meat intake has been associated with gastrointestinal (GI) diseases, including inflammatory bowel disease (IBD), colorectal cancer (CRC) (Rawla et al., 2019), and non-communicable diseases (NCDs) such as diabetes type 2 and coronary heart diseases (Bechthold et al., 2019). On the other hand, *in vivo* studies in mice indicated that plant-based meat analogs, as compared to pork and beef, exhibited lower digestibility, releasing fewer peptides. Consequently, a downregulation of gene expression related to gastrointestinal nitrogen

* Corresponding author at: Assistant Professor in Gastrointestinal Health, Wageningen University & Research, Division of Human Nutrition and Health (Nutritional Biology) & Food Quality and Design, P.O. Box 17, 6700 AA Wageningen. Wageningen Campus, HELIX - Building Stippeneng 4, | 6708, WE, Wageningen, The Netherlands.
E-mail address: josep.rubert@wur.nl (J. Rubert).

https://doi.org/10.1016/j.foodchem.2024.140161
Received 15 December 2023; Received in revised form 28 May 2024; Accepted 17 June 2024
Available online 22 June 2024

nutrient sensors resulted in diminished gastrointestinal digestive functions (Xie et al., 2022). Recent research suggests that pea-based PBMA enhances SCFA production in the Simulated Human Intestinal Microbial Ecosystem (SHIME®) (Zhou et al., 2023). In this frame, an interventional study reveals an increase in butyrate-producing bacteria in individuals consuming pea-based meat compared to other animal protein sources such as red meat, fish, poultry, eggs, and cheese (Toribio-Mateas et al., 2021). These findings align with the growing body of research demonstrating the beneficial anti-inflammatory effects associated with soy and pea-based protein interventions (Raffner Basson et al., 2021). However, the complex inflammatory process of intestinal mucosa could involve various factors, including excessive hydrogen sulfide, lack of indolic compounds and butyrate, and catabolism pathways of phenylalanine, tryptophan, and histidine (Portune et al., 2016).

Colonic microbial communities interact with proteins that escape digestion and absorption in the small intestine, producing an extensive repertoire of GMMs that can significantly influence gut homeostasis. However, current literature comparing the effects of PBMA and real meat on intestinal physiology has predominantly determined SCFAs. Therefore, it is crucial to develop comprehensive analytical methods to assess the changes in GMM profiles that occur during colonic fermentations. Due to the chemical structure of many GMMs, ultra-high performance liquid chromatography coupled with high-resolution mass spectrometry (UHPLC-HRMS) provides a fast, sensitive, and accurate technology for the screening of a virtually unlimited number of GMMs in a single analysis (Vanden Bussche et al., 2015). The use of hybrid HRMS mass analyzers enables the acquisition of data on ionized molecules and fragmented ions in a single injection and, therefore, significantly increases the possibilities for metabolite identification (Lacalle-Bergeron et al., 2021).

This study aims to test the hypothesis that PBMAs and beef patties generate distinct GMM profiles due to protein composition, digestibility, and the delivery of substrates to microbial communities. To evaluate these differences, we conducted *in vitro* experiments mirroring digestion and colonic fermentation. Then, we analyzed the resulting slurries using a comprehensive metabolomics approach. Step by step, firstly, three different protein sources were selected: a beef patty, a commercial PBMA (pea-based meat), and a homemade pea-based meat analog. These patties were cooked and subjected to the INFOGEST protocol to simulate gastrointestinal digestion. The undigested fractions served as starting materials for fecal batch cultures, mirroring colonic fermentation *in vitro*. Stools from five different donors were used to mirror colonic fermentation *in vitro*, collecting samples at different time points (0, 6, 12, 24, and 48 h). An untargeted approach using UHPLC-QTOF MS with reversed-phase (RP) and hydrophilic interaction liquid chromatography (HILIC) aimed to compare chemical fingerprints of protein-related GMMs. The pipeline to process the generated data included several open software packages for data processing, retention time alignment, identification, and statistical analysis. Additionally, SCFA, ammonia, pH, total indole, and phenol content were assessed through target methodologies, which contributed to a comprehensive understanding of the impact of the different protein sources on GMM production.

2. Materials and methods

2.1. Chemicals and reagents

Porcine pepsin (P6887), porcine pancreatin (P1750, 4× USP), and porcine bile salt preparation (B8631) were purchased from Sigma-Aldrich (Merck KGaA, Darmstadt, Germany). KCl, KH_2PO_4, $MgCl_2{\cdot}(H_2O)_6$, $CaCl_2{\cdot}(H_2O)_2$, and pure ethanol were purchased from VWR International B.V. (Amsterdam, Netherlands). Yeast extract, peptone, mucine and L-cysteine HCl, NaCl, $(NH_4)_2CO_3$, $NaHCO_3$, NaOH, HCl, and Tween 80 were purchased from Sigma-Aldrich Chemie NV (Zwijndrecht, Netherlands).

For the preparation of mobile phases for chromatographic analysis, LC-MS grade methanol (MeOH), acetonitrile (ACN), 2-propanol (IPA), and water were purchased from Biosolve B.V. (Valkenswaard, Netherlands). For the rest of the experimental part Milli-Q water was produced by Milli-Q PURELAB Ultra, ELGA LabWater (Lane End, U.K.). Ammonium acetate, ammonium formate, formic acid, and methyl tert-Butyl ether (MTBE) were purchased from Sigma-Aldrich Chemie NV (Zwijndrecht, Netherlands). Internal standards (ISs) were also purchased from Sigma-Aldrich Chemie NV (Zwijndrecht, Netherlands). They were added to the mixtures in the following concentrations: 500 ng mL^{-1} of tryptophan d_5, trans-cinnamic acid d_7, L-Lysine d_4 hydrochloride, 250 ng mL^{-1} of dopamine d_4, and ^{13}C Glycocholic acid-(glycyl-1-^{13}C), and 150 ng mL^{-1} of acrylamide-d_3.

2.2. Patty material

A beef patty (125 g) was purchased from Slagerij Elings B.V. (Wageningen, The Netherlands), consisting of 80% lean beef meat and 20% beef fat; this patty is labeled as RM. An available plant-based commercial patty labeled as PBCB was obtained from the local supermarket Albert Heijn (Wageningen, The Netherlands). Given that the commercial PBMA contains other ingredients such as emulsifiers, flavor enhancers, and dietary fibers, among others, a homemade PBMA without food additives was introduced as a control. For the homemade patty, labeled as PP, pea protein isolate was provided by Ingredion (Hamburg, Germany), and coconut oil was purchased from Thermo Fisher Scientific (Breda, Netherlands). The protein, fat, and water ratios were similar in the three products. More details on the composition of the foodstuff material can be found in **Table S1**. The three patty types were baked in a conventional oven for 6–10 min at 180 °C until the core reached 60 °C. All samples contained the same amount of water (More details in the Supporting Information, Section 1.1).

2.3. Simulated in vitro gastrointestinal digestion

The three baked patties were digested using the INFOGEST method (Brodkorb et al., 2019), which consists of a simulated oral, gastric, and intestinal phase with modifications. The compositions (%, *w*/w) of the simulated salivary fluid (SSF), simulated gastric fluid (SGF, pH 3.0 ± 0.05), and simulated intestinal fluid (SIF, pH 7.0 ± 0.05) were as reported in previous works (Huyan et al., 2022). The entire process was carried out at a constant temperature of 37 °C and with 5 replicates per patty (More details in the Supporting Information, Section 1.2). At the end of the process, samples were incubated for 2 h on a rotating device. Control samples were prepared using the same procedure without any digestive enzymes, adding MilliQ H_2O instead. All the collected fractions were centrifuged to halt the enzymatic process (4 °C, 20000 g, 10 min). Finally, 25 mL of supernatants were collected for further analysis, while pellets were freeze-dried and pooled to be used as undigested samples for the *in vitro* colonic fermentation.

2.4. Fecal Donors

The composition of microbiota varies significantly among individuals, making interventions highly dependent on each individual's basal state. For this reason, it is necessary to select a representative number of fecal donors to ensure unbiased results (Isenring et al., 2023). In the current study, five healthy fecal donors were selected. The volunteers were 25–45 years of age, non-smokers with a BMI of 18.5–25, located in Wageningen (NL) and its surroundings. As exclusion criteria, all the volunteers must not have received antibiotic treatment 3 months before stool collection, must not have consumed pre- or probiotic supplements before the experiment, and must not have a history of bowel disorders. Participants were informed about the study research, and written consents were obtained. According to the Medical Ethical Advisory Committee of Wageningen University (METC-WU) guidelines, this research is exempted from ethical approval. The participants are not

subjected to acts regulated by METC-WU.

2.5. In-vitro batch fermentation

Colonic fermentation was carried out based on previously reported protocols, with some modifications (Huyan et al., 2022). All the information relevant to *in vitro* fermentation has been included in the Supporting Information (Section 1.3.). Briefly, Fecal Microbiota Supernatant (FMS) was prepared by homogenizing 40.0 g of fresh feces (five donors) in 200 mL of anaerobic phosphate buffer using a stomacher bag, and a buffered colon medium consisting of different amounts of K_2HPO_4, $NaHCO_3$, yeast extract, peptone, mucin, L-cysteine, and Tween 80. The undigested fractions of the *in vitro* gastrointestinal digestion, named pellets, were mixed with buffered colon medium and FMS in 10 mL glass water-jacketed vessels. Batch cultures were incubated at 37 °C for a period of 48 h, and slurries were taken at different time points (0, 6, 12, 24, and 48 h); for donors 3, 4, and 5, slurry fractions were also collected at 3 and 32 h. It is important to note that static models are discontinuous. Once colonic fermentation begins, there is no further input of substrates, and the products of microbial metabolism accumulate. This leads to a change in environmental conditions that can stop microbiota activity and growth. Therefore, the fermentation process cannot extend beyond 48 h. The chosen time intervals provide a snapshot of the GMMS changes during this period. The most important changes are expected to occur in the first hours, which is why the intervals are shorter at the beginning of digestion. All slurry fractions were centrifuged and quenched with liquid N_2 immediately after sampling and stored at −20 °C until further use. A total of 8 fermentations were performed per donor: the three digested patties with FMS, the three digested patties without FMS (blank samples), and two blanks of the fermentation process, with and without FMS. More details about sample composition and assigned labels can be found in **Table S.2**.

2.6. A rapid biochemical profiling comparing red meat and meat analogs

2.6.1. Ammonia determination

A colorimetric assay kit (Ammonia Assay Kit AA0100, Sigma-Aldrich, St. Louis, USA) was used to analyze the ammonia content in the samples. To make sure the ammonia content was within the detection range of the kit, a 3× dilution factor with MilliQ H_2O was used. Additionally, materials were clarified by centrifuging them (4 °C, 12,557 g, 10 min) using an Eppendorf 5430R centrifuge. Then, a microplate spectrometer (SpectraMax ABS Plus, Molecular Devices, San Jose, USA) was used to measure the supernatant absorbance at 340 nm.

2.6.2. Total phenolic content

A colorimetric assay kit (Phenolic Compounds Assay Kit MAK365, Sigma-Aldrich, St. Louis, USA) determined the total phenolic content. Pre-experiment data showed no dilution was needed to bring total phenolic content to appropriate measuring ranges. Absorbance was measured at 480 nm using a microplate spectrometer (SpectraMax ABS Plus, Molecular Devices, San Jose, USA).

2.6.3. Indole analysis

A colorimetric assay kit determined the total indole content (Indole Assay Kit MAK326, Sigma-Aldrich, St. Louis, USA). Before measurement, samples (150 µL) were diluted with 450 µL MilliQ H_2O and centrifuged (4 °C, 12,557 g, 10 min) using a 5430R Eppendorf centrifuge. 100 µL of the supernatant was used further for the analysis. The absorbance was measured at 565 nm using a microplate spectrometer (SpectraMax ABS Plus, Molecular Devices, San Jose, USA).

2.6.4. pH measuring

The pH measurement of all samples was performed using a pH electrode (VWR® PHenomenal® PH 1000 L). Before performing the measurement, the pH meter was calibrated. The process for preparing the sample involved mixing it in a vortex for 30 s before dissolving 0.5 mL of it in 4.5 mL of deionized water. The pH of the dilution was then measured.

2.6.5. SCFAs analysis

The fermentation supernatants were subsequently centrifuged (4 °C, 12,557 g, 5 min) and 2 mL were filtered (15 mm ∅, 0.2 µm regenerated cellulose filter, Phenomenex, Torrance, USA). Then, an internal standard of 2-ethylbutyric acid in 0.3 M HCl and 0.9 M oxalic acid was also added before injection into a gas chromatography system equipped with a flame ionization detector (GC-FID, GC-2014, Shimadzu, Hertogenbosch, Netherlands). The carrier gas employed was nitrogen. The temperature of the ramp of GC-FID started at 100 °C, then increased to 180 °C at a rate of 10.8 °C min^{-1} and held at this temperature for 2 min. Then, it increased to 240 °C at a rate of 50 °C min^{-1} and was maintained at this temperature for 2 min. Standard calibration curves for acetic, propionic, butyric, valeric, isobutyric, and isovaleric acids were created in the 0–50 mM concentration range.

2.7. Untargeted metabolomics approach

2.7.1. Sample preparation

The extraction protocol was designed to obtain the non-polar and polar fractions of the samples from the *in vitro* gastrointestinal digestion (INFOGEST) and the colonic fermentation (*CF*). The current dual extraction method was adapted from previous studies with fecal samples (Deda et al., 2015; Talavera Andújar et al., 2022). The digestion sample flasks were thawed and vortexed for one minute, and then 100 µL of the homogenized sample was transferred into separate Eppendorf tubes. The sample was homogenized with 1 mL of MilliQ H_2O:MeOH (1:1, *v*/v), and vortexed (90 s), followed by sonication (10 min) at low temperature. Then, a liquid-liquid extraction (LLE) was performed for the separation of the polar and the non-polar analytes by adding 600 µL MTBE. Additionally, 120 µL of IS was added to each sample. Three cycles of vortex (30 s) and incubation in a refrigerator (5 min) were performed to ensure the proper transfer of the metabolites. Afterward, the samples were centrifuged (4 °C, 12,557 g, 10 min), and then, 300 µL of the upper organic phase and 1 mL of the polar fraction were transferred to glass vials. Glass vials with polar fractions were transferred to a Christ rotational vacuum concentrator System (LabMakelaar Benelux B.V., Zevenhuizen, Netherlands) to evaporate the solvents to dryness. For the evaporation of the organic solvent in the non-polar fractions, the vials were placed in a fume hood overnight, in the dark, and at room temperature. All vials were capped and stored at −80 °C before the reconstitution and analysis. The dried polar fractions were reconstituted with 150 µL of MilliQ H_2O:MeOH (9:1 *v*/v) in 0.1% FA. Afterward, the tubes were vortexed (90s), sonicated (10 min), and centrifuged (4 °C, 12,557 g, 10 min). Finally, the samples were transferred into insert LC-MS vials. Quality control (QC) samples were prepared by mixing 15 µL of all samples. Blank extraction samples were included following the same procedure. The instrument performance was monitored by using ISs and QCs

2.7.2. UHPLC-HRMS

The polar fraction analysis (5 µL) was carried out with a Nexera XS UHPLC system (Shimadzu Corporation, Kyoto, Japan) coupled to an LCMS-9030 quadrupole time-of-flight mass spectrometer (Shimadzu Corporation, Kyoto, Japan). The UHPLC unit consisted of a SIL-40C XS Autosampler, an LC-40D XS solvent delivery pump, a DGU-405 degassing unit, a CTO-40S column oven, and a CBM-40 lite system controller. The QTOF-MS system was equipped with a standard electrospray ionization (ESI) source unit and a calibrant delivery system (CDS). The analysis was carried out in Hydrophilic Interaction Liquid Chromatography (HILIC) and reversed-phase liquid chromatography (R. P.) to analyze polar and medium polar compounds. A SeQuant® ZIC®-HILIC 5 µm particle size analytical column 150 × 4.6 mm (Merck KGaA,

Darmstadt, Germany) and an Acquity UPLC BEH C18 column 1.7 μm particle-sized analytical column 2.1 × 100 mm connected to an Acquity UPLC BEH C18 VanGuard Pre-column, 130 Å, 1.7 μm, 2.1 mm × 5 mm (Waters Chromatography B.V., 4879 AH Etten-Leur, the Netherlands), were used for the HILIC and the R.P. analysis, respectively. The HILIC elution was performed using ACN (mobile phase A) and H_2O (mobile phase B) in 0.1% HCOOH and 10 mM NH_4HCOO. The gradient started with 90% of A until 3.0 min, 70% of A at 5.0 min, 20% of A at 11 min, 20% of A at 17 min, and 90% of A at 20 min with a total run time of 20 min and 0.7 mL min^{-1}. For R.P. separation, H_2O (mobile phase A) and MeOH (mobile phase B), both with 0.1% HCOOH, were used. The gradient started from 10% B at 0 min to 90% B at 14 min, 90% B at 16 min, and 10% B at 16.01 min with a total run of 18 min and a flow rate of 0.3 mL min^{-1}. A total of 3 analyses were performed for both INFOGEST and *CF*: HILIC and RP in positive ionization and RP in negative ionization. The column oven was set at 40 °C in all the acquisitions. Samples were randomly injected into the UHPLC-QTOF MS system with the aim of reducing the bias due to potential instrumental drift. The sample list was arranged as follows: the sequence begins with 5 extraction blanks, followed by 10 QC injections that stabilize the column. Thereafter, one QC and one extraction blank were injected into every ten and twenty samples, respectively.

The voltage of the ion-spray ionization was 4.0 kV and − 3.0 kV for ESI+ and ESI-, respectively. For both negative and positive ionization, the heat block, desolvation line, and electrospray ionization probe temperatures were set at 400 °C, 250 °C, and 300 °C. At the same time, the flow rates were 2 mL min^{-1} for the nebulizer gas and 10 mL min^{-1} for the heating and drying gas. For data-dependent acquisition (DDA) analysis, MS^1 and MS^2 were acquired over an *m/z* range of 50–1000 Da and 100-1000 Da, respectively. The number of DDA events was set to 18 with an event time of 0.05 s and a total loop time of 1 s, and the charge states were set between 1 and 3. Automatic exclusion of ions was performed by excluding other isotopes, ions of other charge states, and background artifact ions using a homemade exclusion list. The signal threshold was set at 1000, while the collision-induced dissociation (CID) energy ramp was set from 18 to 52 eV, with a gas pressure of 230 kPa. The mass axis and tune parameters were calibrated weekly with a sodium iodide (NaI) solution (Standard Sample for LCMS-9030, Shimadzu Corporation, Kyoto, Japan). All the acquired mass spectra were internally calibrated by injecting ESI-L Low Concentration Tuning Mix (Agilent Technologies Netherlands BV, Amsterdam, Netherlands) through the sub-interface at the end of the run (equilibrating conditions).

2.7.3. Data processing

UHPLC-QTOF MS raw data files were imported into MS-DIAL (MS-DIAL software, version: (MS-DIAL software, version: 4.9.2.2, Japan) for baseline filter, peak detection, retention time alignment, and annotation (Tsugawa et al., 2015). Automated feature detection was performed from 0.5 min to 16 and 17 min for RP and HILIC, respectively. In all the analyses, mass signal extraction ranged from 50 to 1000 Da, while MS^1 and MS^2 tolerances were set to 0.01 and 0.03 Da, correspondingly. The minimum detection thresholds were set at 1000 and 10 for MS^1 and MS^2, respectively. For alignment purposes, a QC from the middle of the sequence was selected as a reference file. The retention time tolerances were set at 0.2 and 0.5 min for R.P. and HILIC, subsequently. After deconvolution, deconvoluted and annotated peaks were transferred to Excel to generate a matrix of *m/z* ratios, retention times, peak intensities, and MS/MS spectra of the deconvoluted ions. Features present in extraction blank, without MS/MS assigned, *m/z* match, or MS/MS match were removed. In addition, those that showed low repeatability in the blanks of the fermentation process without fecal microbiota were discarded. Low repeatability was determined by using the RSD (>50%). The average of the blank samples was more than one-tenth of the average of the feature in the groups with sample (RM, PBCB, and PP), to avoid discarding those features close to the limit of detection (LOD) in the group of blank samples.

MetaboAnalyst 5.0 was used to perform the data filtering and statistics. To remove features with low repeatability or close to the baseline features with RSD > 25% in QC and interquartile range (IQR) < 40% were discarded, respectively. Once the data set was filtered, the statistical study was focused on the metabolic variation between the two commercially available protein sources: RM and PBCB. For INFOGEST samples, one-factor statistical analysis was used to highlight the metabolic differences between both groups. In the case of colonic fermentation samples, it was interesting to explore these changes across the different time points of the colonic fermentation. Therefore, the option *time series + one factor* was selected for this purpose. Multivariate Empirical Bayes Time-series Analysis (MEBA) was used to rank features according to Hotelling's T2 value, which indicates the differential temporal profiles. GraphPad Prism 10 (GraphPad Software, La Jolla, CA) was used to represent the results graphically. The findings were expressed using the mean values ± standard error of the mean of transformed data (square root, (SEM, $N = 5$), and differences were evaluated using two-way repeated analysis of variance (ANOVA), considering a value of $p < 0.05$ statistically significant.

2.7.4. Compound annotation

All openly accessible MS/MS spectral MSP-formatted libraries (MSPs) were used to tentatively annotate features during data processing. By the time this study was conducted (March 2023), these databases included 16,995 and 15,245 unique compounds for positive and negative ionization, respectively. Additionally, data processed with MS-DIAL, including unknown features, were exported to GNPS (Wang et al., 2016) for Feature-Based Molecular Networking (FBMN) to enhance the annotation with GNPS spectral libraries (Nothias et al., 2020). Those features without MS/MS fragmentation were discarded.

The identification confidence level system introduced by Talavera Andújar et al. (Talavera Andújar et al., 2022) was used to classify the features annotated by MS-DIAL. The *Dot product* parameter enabled the assessment of the quality of the match between the different samples and spectra in each MS/MS dataset. *In silico* fragmentation platform *MetFrag* (Ruttkies et al., 2016) was used to confirm the MS/MS ion fragments matching. Those features whose annotations could not be explained were also discarded.

3. Results and discussion

3.1. In vitro bioavailability differences between beef and plant-based patties in the small intestine

Foods undergo significant changes before reaching the colon, food integrity is compromised, and some macromolecules are hydrolyzed during digestion. The present study performed simulated gastrointestinal digestion employing the INFOGEST protocol (Brodkorb et al., 2019), as a standardized methodology to simulate upper gastrointestinal digestion, followed by a colonic fermentation model. The primary goal of using this methodology was to provide a substrate for the subsequent colonic fermentation studies. Additionally, the supernatant from the intestinal phase was assessed since it provides valuable information about compounds that are rapidly absorbed by intestinal epithelial cells in the small intestine.

Untargeted metabolomics was applied to compare fingerprints of annotated metabolites that changed in response to the different feeding conditions (*See Supplementary Materials, Section 2.1 and* ***Fig. S.1***). Univariate and multivariate statistical analyses were then applied to investigate the metabolic differences between the different feeding conditions. Only those features that met the following characteristics were chosen *t*-test (p-value<0.05), volcano plot (p-value<0.05), fold-change>2, OPLS-DA (pcorr>|0.8| and p[1] > |0.1|). The selected markers, including 32 markers of RM and 45 markers of PBCB, are recorded in **Table S.3**. Among the features highlighted for beef meat

digested samples, it is noteworthy to mention the presence of carnitine and acylcarnitines such as acetylcarnitine, butyryl carnitine, propionyl carnitine, hexanoyl-L-carnitine. Carnitine and derivates are known biomarkers of beef consumption, and they have essential roles in energy production by lipid β-oxidation in the mitochondria of muscle cells in mammals (Israr et al., 2021). Other known red meat markers found in beef patties were L-carnosine, L-anserine, taurine, creatine, and acylcholine (Cuparencu et al., 2019). Triterpene and steroidal saponins, triterpenoids, oligosaccharides, flavones, lignans, and purine and purine derivates were the compounds found in the intestinal fraction of the digested plant-based commercial analog, which are compounds naturally found in pea beans (Sri Harsha et al., 2018).

Among the amino acids found in RM, alanine, glutamine, leucine, lysine, methionine, phenylalanine, tryptophan, and valine were the most abundant, while proline and asparagine were more predominant in PBCB. According to the food matrix characterization performed by De Marchi et al., the average amino acid composition in plant-based patties (pea and soy) is quite similar to meat-based patties. However, PBMA presented low methionine, glycine, and lysine levels but high glutamic and aspartic acid levels compared to the animal-based option (De Marchi et al., 2021). Consequently, the findings of the current study suggest that the composition of the food matrix potentially affects amino acid release in the small intestine, which is particularly higher in patties of animal origin. In this regard, *in vivo* studies on mice showed that consuming animal-based patties increased the transfer of essential and non-essential amino acids from the jejunum to the bloodstream compared to the digestion of their PBMA counterpart (Xie et al., 2022). Xie et al. also reported variations in the peptide composition resulting from the digestion of both patties. Although proteomics is beyond the scope of our study, differences in the levels of small peptides, such as di- and tri-peptides, were also identified.

3.2. Modeling the impact of undigested proteins in the colonic region

The undigested fraction generated during the final stage of the simulated gastrointestinal digestion was employed as substrate for the *in vitro* colonic fermentation model, with 233 samples collected longitudinally. The final list of collected samples is compiled in **Table S.4**. A thorough assessment of these samples is crucial for understanding the intricate interactions between undigested proteins, peptides, and free amino acids with the gut microbiota, ultimately shedding light on their impact on gastrointestinal health. Untargeted metabolomics based on LC-QTOF MS offers a comprehensive and unbiased approach to assessing the changes in GMMs produced during colonic fermentation. However, there are relevant protein-derived GMMs that are outside the scope of LC-QTOF MS, such as SCFA, ammonia, and H_2S. To address this limitation, targeted approaches were implemented to assess these metabolites. Additionally, total phenol and indole content were measured through available commercial kits, as their presence, derived from the fermentation of aromatic amino acids, can significantly influence epithelial cell viability and proliferation, barrier functionality, and immune response (Portune et al., 2016).

3.2.1. A rapid biochemical profiling comparing red meat and meat analogs

3.2.1.1. Ammonia, total phenol content, indoles, and pH. Ammonia, comprising NH_4^+ and NH_3, is produced by the bacterial deamination of amino acids and is highly sensitive to changes in the intestinal environment. High-protein diets are associated with increased ammonia concentrations, and excess amounts can inhibit SCFA oxidation in the colonocytes (Blachier et al., 2017). During the initial 6 h of fermentation, ammonia levels increased evenly for all protein sources before stabilizing, and no significant differences were observed between different protein sources (Fig. 1.**A**).

Phenolic compounds present in the colon can be obtained through the fermentation of plant-derived polyphenols or the tyrosine catabolism pathway. Given the protein-rich and carbohydrate-poor nature of the samples in the current study, most phenol species are suspected to correspond to tyrosine metabolites like p-cresol, phenol, and 4-ethylphenol (Portune et al., 2016). These phenolic compounds might exert genotoxicity on human colonocytes, inhibiting their proliferation and viability (Blachier et al., 2017). At time zero, RM, PBCB, and the blank

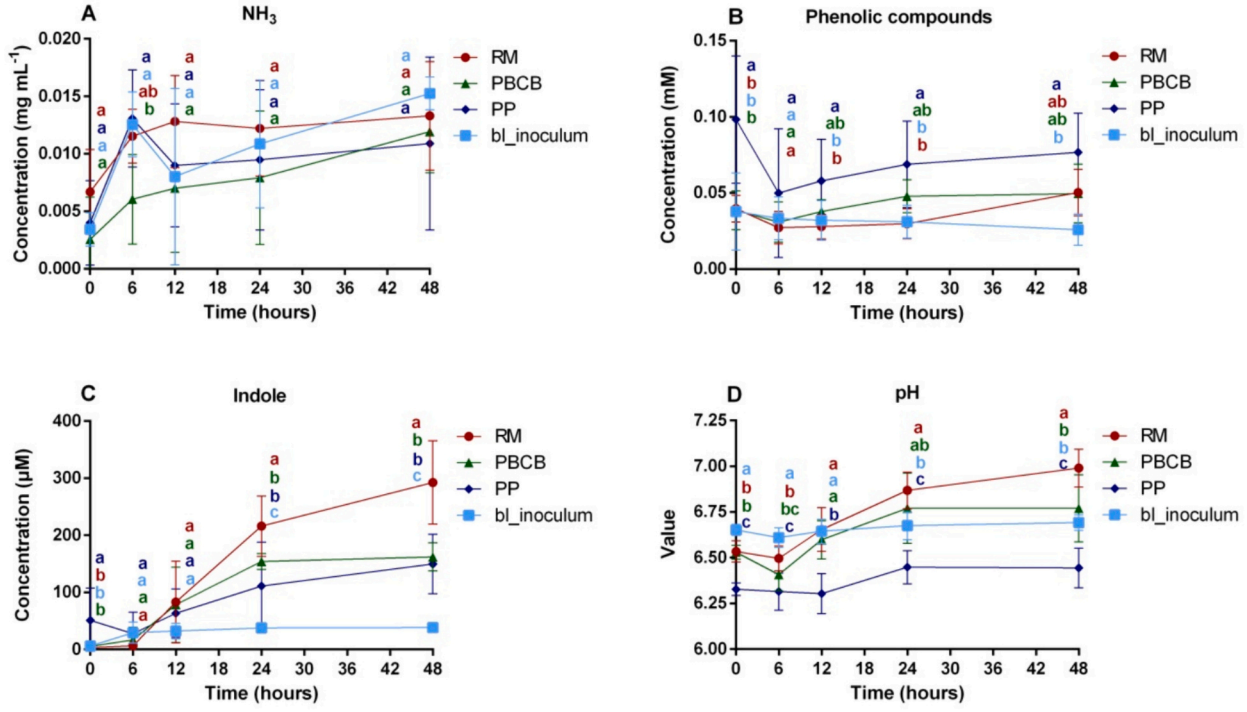

Fig. 1. The concentrations of ammonia, total phenolic compounds, total indoles, and pH (A-D) during the *in vitro* colonic fermentations. Blank inoculum, RM, PBCB, and PP samples are depicted. The different letters indicated the significant difference by One-way ANOVA analysis for different groups at the same time point.

inoculum exhibited comparable levels, whereas PP displayed significantly higher total phenol content. However, this difference became less pronounced toward the end of the fermentation process (Fig. 1.**B**).

Indole and its derivatives are derived from the metabolism of tryptophan by gut microorganisms. Indoles have been shown to increase the expression of tight-junction proteins in the gut epithelium, thereby improving intestinal barrier function and reducing inflammatory markers (Portune et al., 2016). Cumulative indole levels gradually increased over time (Fig. 1C). During the initial 12 h of fermentation, the indole content was similar across all the protein sources. Subsequently, indole production increased, particularly in the RM group, which exhibited higher levels by the end of the fermentation period.

Organic acids (*e.g.*, SCFA), hydrogen sulfide, and ammonia influence luminal pH. Reciprocally, pH can modulate microbial communities and the effects of metabolites. As a general trend, the pH increased throughout the colonic fermentation, ranging between 6.1 and 7.5 (Blachier et al., 2017). Similar trends were observed in the current study for the protein sources (Fig. 1.**D**). Markedly, plant-based samples yielded a lower pH than meat protein by the end of the fermentation, potentially reducing hydrogen sulfide concentration, which might

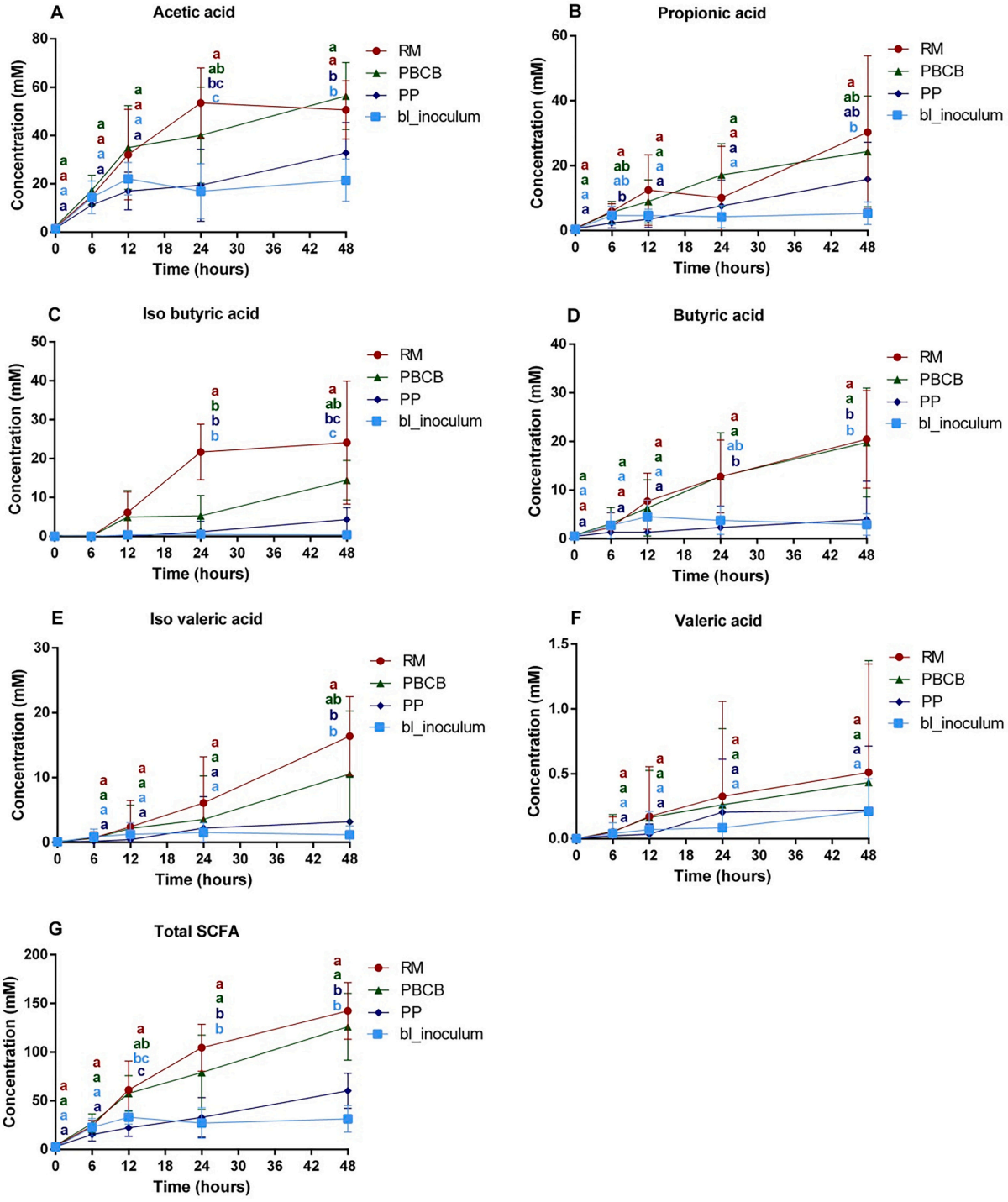

Fig. 2. Concentrations of individual SCFAs and total SCFAs (A–G) for blank inoculum, RM, PBCB, and PP samples. The significant difference analysis for different samples at the same time point. The different letters indicated the significant difference by One-way ANOVA analysis for different groups at the same time point.

inhibit colonocyte oxygen consumption. It is worth mentioning that the pH of the PP group was substantially lower than the rest of the groups, including the blank without a feeding condition (blank inoculum). This could be caused by the low production of SCFAs for the PP group (*See Section 3.2.1.2*).

3.2.1.2. SCFA. While SCFA and BCFA typically result from carbohydrate fermentation, they can also be originated from amino acids by reductive deamination. Fig. 2 depicts the concentration (mM) of acetic acid (Fig. 2**.A**), propionic acid (Fig. 2**.B**), isobutyric acid (Fig. 2**.C**), butyric acid (Fig. 2**.D**), isovaleric acid (Fig. 2**.E**), valeric acid (Fig. 2**.F**) and the sum of SCFAs (Fig. 2**.G**) during the colonic fermentation. As a general trend, the production of SCFA increased for RM and PBCB samples after 6 h, with minimal differences observed between these two groups for the remaining fermentation points (Fig. 2**.G**). This distinction is particularly evident in the production of isobutyric and isovaleric acid (Fig. 2**.C and 2.D**, respectively). The total SCFA production in the homemade plant-based patty remained similar to the blank in all cases, maintaining its concentration lower than that of PBCB and RM samples after 48 h of fermentation. One possible explanation for the differences lies in the processing conditions of both pea proteins. The varying structures of texturized proteins can impact their digestibility and the availability of amino acids for the gut microbiota. This, in turn, can interfere with the production of other gut microbial metabolites, as well as the addition of dietary fibers.

3.2.2. Protein-related GMMs elucidated by an untargeted metabolomics workflow

Samples were extracted and analyzed following the untargeted metabolomics approach designed for polar and semi-polar metabolites (*See Section 2.6.1*). After data processing, annotation, and data filtering, a total of 343 features for HILIC ESI (+), 306 for RP ESI (+), and 157 for RP ESI (−) were collected. QC pool grouping in the PCA score plot (**Fig. S.2**) indicates adequate analytical performance across all three acquisitions. **Fig. S.2** shows that the highest degree of dispersion was given within groups containing undigested substrate and fecal inoculum (RM, PBCB, and PP). However, PCA or supervised multivariate models as partial least squares discriminant analysis (PLS-DA) are inadequate models to evaluate the metabolic changes in a time-series metabolomics, in contrast to alternative approaches like MEBA, which provides a valuable tool for assessing the variability of both, within and between time points (Xia et al., 2011). This approach was used to rank the potential metabolites of interest according to their Hoteling's T2 value by comparing RM and PBCB groups across the colonic fermentation and selecting only those features with a Hoteling T2 > 20. Special attention was paid to removing non-informative markers before modeling the data. First, those features showed low repeatability in both QC replicates and blanks of the fermentation process without fecal inoculum. Second, variables that were almost constant across the experiment conditions and those with a signal close to the baseline. **Table S.5** collects all the selected annotated features through the untargeted metabolomics workflow sorted out by ontology together with the level of identification. Among the families of compounds highlighted through the metabolomics pipeline were amino acids and derivates, acetylated amino acids, dipeptides, and hybrid peptides. The combination of RPLC and HILIC was useful to cover a broader range of polarities and expand the metabolic scope of the study. For example, the elucidation of highly polar compounds, such as acetylated amino acids, would not have been possible without using HILIC. The following sections describe the trends observed for every chemical family and discuss their potential implications on the intestine. The alterations in metabolite profiles resulting from *in vitro* colonic fermentation are attributed to the influence of the gut microbiota. Therefore, we use the terms anabolism and catabolism to denote the constructive (biosynthetic processes) and destructive (breakdown and utilization of molecules) metabolic pathways, respectively.

3.2.2.1. Trends in amino acids and derivates comparing red meat and meat analogs. Among all the annotated amino acids, only phenylalanine, methionine, tyrosine, and tryptophan (Fig. 3**.A, 3.B, 3.C, and 3.D,** respectively) exhibited notable differences between RM and PBCB during colonic fermentation. It is worth noting that the inoculated samples without substrate (bl_inoculum) displayed high basal levels of amino acids due to the medium composition (*See Section 2.5*). Phenylalanine was released during colonic fermentation in beef and pea-based patties, with slightly higher levels in the second group. As expected, RM stood out from the rest at basal levels of methionine, experiencing more accelerated catabolism than the rest of the groups at 12 h. The ANOVA analysis, which is more restrictive than the MEBA, did not show significantly different trends in tyrosine and tryptophan levels between RM and PBCB throughout colonic fermentation. However, PP exhibited greater concentrations of both amino acids at the end of the process. Increased bioavailability of tyrosine could promote the production of phenols in this group (*See Section 3.2.1.2*). As the correlation between tryptophan and the total indole content (*See Section 3.2.1.3*) is not so evident, the findings of this study suggest that other factors could be involved.

3.2.2.2. Histidine and proline derivates. The phenylalanine, tryptophan, and histidine metabolomic pathways are closely related to gut inflammation (Xu et al., 2022). Although no relevant derived metabolites were found through the metabolomics pipeline for phenylalanine and tryptophan, a histidine derivative methyl-histidine (Fig. 3**.E**) was discovered, exhibiting a distinct trend in beef patty samples during the initial 24 h of fermentation. Even though histidine was not highlighted in the MEBA analysis (**Fig. S.3.A**), its methylation can occur at either the N1 or N3 position of its imidazole ring, resulting in 1-methyl (1-MH) and 3-methyl histidine (3-MH) (Moro et al., 2020). Both isomers, 1-MH and 3-MH, can only be produced from histidine residues by methyltransferases in mammals (Davydova et al., 2021). 3-MH, as a part of the histidine metabolic pathway, may have a role in inflammation diseases. However, the association was not established in stool on a mouse model (Xu et al., 2022). A recent *in vivo* analysis of feces discovered lower amounts of 3-MH and anserine (*See Section 3.2.2.2*) in patients with irritable bowel syndrome (Liu et al., 2023).

Regarding the proline derivatives, two distinctive features were annotated as hydroxyproline: hydroxyproline I, measured in RP ESI (+), and hydroxyproline II in HILIC ESI (+). In both cases, two crucial structural fragment ions were identified: m/z 86.0606 and m/z 68.0500, both associated with the pyrrolidine structure of the proline, displaying differing trends. Hydroxyproline I (**Fig. S.3.B**) showed the same basal level for all the groups. Conversely, a substantial amount of hydroxyproline II (Fig. 3**.F**) was observed in the RM group. Hydroxyproline I demonstrated an increase during the first 12 h of fermentation. In contrast, hydroxyproline II appeared to undergo catabolism by gut microbiota. This hydroxyproline may correspond to 4-hydroxyproline, a well-known biomarker of red meat that serves as a prominent constituent of protein collagen, contributing significantly to collagen stability. This proline derivative is recognized for its beneficial effects on bone, joint, and skin stability, with specific animal models revealing its role in preventing gut inflammation (Wu, 2020). Previous studies in rats have suggested that most of the 4-hydroxyproline present in the bloodstream originates from free 4-hydroxyproline and 4-hydroxyproline-containing di- and tri-peptides whose hydrolysis takes place by enterocytes (Osawa et al., 2018). However, there is no evidence of being metabolized by gut microbiota. While 4-hydroxyproline is known to play a significant role in the metabolic pathway for glycine production, its catabolism remains poorly understood. The findings of our study shed light on the potential role of the gut microbiota in the utilization of 4-hydroxyproline, thereby paving the way for further exploration in this area.

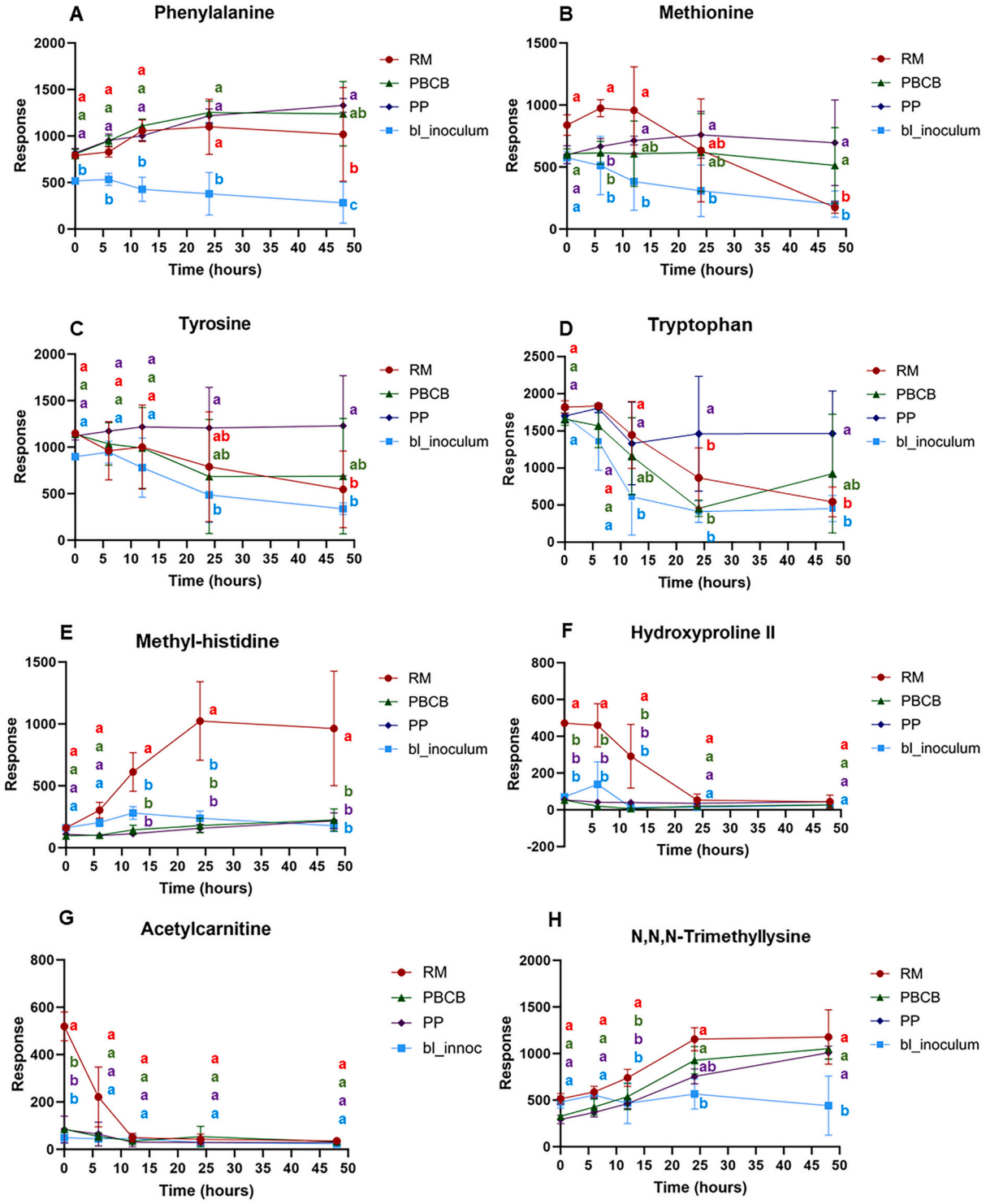

Fig. 3. Response of (A) phenylalanine, (B) methionine, (C) tyrosine, (D) tryptophan, (E) methyl-histidine, (F) hydroxyproline II, and (G) acetylcarnitine, (H) *N,N,N*-Trimethyllysine. Notes: RM beef patty, PBCB plant-based commercial patty, PP plant-based homemade patty, bl_inoculum, sample without any substrate. The different letters indicated the significant difference by two-way ANOVA analysis for different groups at the same time point.

3.2.2.3. TMAO biosynthesis pathway. *L*-acetylcarnitine was initially detected at elevated levels in the RM samples at 0 h, but it was rapidly consumed during the colonic fermentation (Fig. 3.**G**). Chemically, acetylcarnitine represents the acetylated derivative of the amino acid L-carnitine, acquired through animal-derived meat consumption (*See Section 3.1*). *L*-acetylcarnitine is commonly associated with regulating energy metabolism within the mitochondria and serves as a substrate in the trimethylamine N-oxide (TMAO) biosynthesis pathway. Trimethylamine (TMN), generated by gut microbes using L-carnitine and choline as substrates, is subsequently converted into TMAO in the liver. Elevated TMAO levels have been associated with an increased risk of cardiovascular disease and heart failure (Israr et al., 2021; Koeth et al., 2019). Regrettably, the low molecular mass of TMN precluded its identification through our untargeted metabolomic approach. Despite the absence of acetylcarnitine and carnitine in plant-based meat substitutes, our findings suggest the production of trimethyllysine (Fig. 3.

H), a component of the TMAO biosynthesis pathway (Maas et al., 2020), during fermentation. Across all the groups under study, *N*,*N*,*N*-trimethyllysine exhibited a consistent basal level and increased during fermentation. The escalation was more pronounced in the RM group during the initial 12 h of fermentation, although these levels were comparable to those of plant-based patties after 24 h. *N*,*N*,*N*-trimethyllysine is formed through protein lysine methylation and plays an important role in carnitine biosynthesis and epigenetics (Maas et al., 2020). To the best of our knowledge, this study provides the first evidence of the anabolism of trimethyllysine during colonic fermentation. The hydrolysis of dietary methylated proteins may contribute to the production of trimethyllysine (Zong et al., 2022)

3.2.2.4. Gut derived N-acyl amides. N-acyl amides were annotated by the metabolomics workflow, as Fig. 4 shows. N-acyl amides are fatty acid molecules characterized by a fatty acyl group linked to a primary amine metabolite *via* an amide bond. The N-acyl amides identified included phenylalanine linkages with caprylic, linoleic, and α-linoleic acid (Fig. 4.**A**, **4.B**, and **4.C**, respectively), and leucine with linoleic acid (Fig. 4.**D**). A significant release of these compounds is observed in the PBCB group throughout colonic fermentation. This trend is less pronounced in the PP group, apart from N-caprylyl-*L*-phenylalanine (Fig. 4.**A**), where the production of this N-acyl amide is particularly higher. The availability of fatty acids may influence the production of N-acyl amides. Despite efforts to mimic PBCB in PP patties, differences in fat sources exist. The PBCB ingredients comprised coconut and canola oil, while PP solely utilized coconut oil. Canola oil is richer in linoleic and α-linoleic acid but comparatively poorer in caprylic acid. Moreover, plant-based commercial patties contain higher levels of caprylic, linoleic, and α-linoleic acid than meat-based ones (De Marchi et al., 2021). Considering the production of N-acyl amides by the gut microbiota, these substances are recognized as crucial in regulating the physiology of the gastrointestinal tract (Cohen et al., 2017). Consequently, elevated levels of these compounds may positively impact gut health.

3.2.2.5. Catabolism of dipeptides and hybrid peptides. Several dipeptides have been highlighted in the elucidation workflow (Fig. 5), revealing two primary trends. (i) Most dipeptides exhibited high levels due to the employed feeding conditions at the beginning of the fermentation, except for the high basal levels of pyroglutamic-(iso)leucine derived from the gut microbiota. (ii) The gut microbiota catabolized all dipeptides during the initial 12–24 h of fermentation. Arginine-(iso)leucine, lysine-(iso)leucine, and pyroglutamyl-(iso)leucine (Fig. 5.**A**, **5.B**, and **5.C**) displayed identical levels at the onset across all feeding conditions, while alanine-(iso)leucine, histidine-(iso)leucine, (Fig. 5.**D** and **5.E**) exhibited heightened levels in the RM group. Conversely, phenylalanine-arginine (Fig. 5.**G**) was exclusively present in plant-based alternatives, while isoleucine-methionine (Fig. 5.**F**) was identified solely in beef meat. A similar trend was observed for the hybrid peptide L-carnosine (Fig. 6.**A**) and, to a lesser extent and not in all donors, for L-anserine (Fig. 6.**B**). Studies have suggested that L-carnosine is an antioxidant for intestinal epithelial cells (Shimizu & Son, 2007). Additionally, its supplementation has been associated with reduced glucose levels, blood pressure, and obesity in rats with metabolic syndrome (Al-Sawalha et al., 2019). Previous research has reported decreased di- and tripeptides along the colon during digestion (Folz et al., 2023). Studies have highlighted the significant role of anserine, a dipeptide containing beta-alanine and 3-methyl-histidine, in promoting intestinal health. This includes preventing gut microbiota dysbiosis, facilitating the repair of the intestinal epithelial barrier, and promoting the production of SCFAs (Han et al., 2021). Peptides derived from protein digestion are suspected to be essential in transmitting signals to gastrointestinal cells and stimulating the intestinal tract (Waldum et al., 2014). A recent study investigating the effects of PBMA intake on the GI digestive function of mice revealed that ingesting PBMA led to reduced peptide production along the small intestine and less efficient gastrointestinal digestion

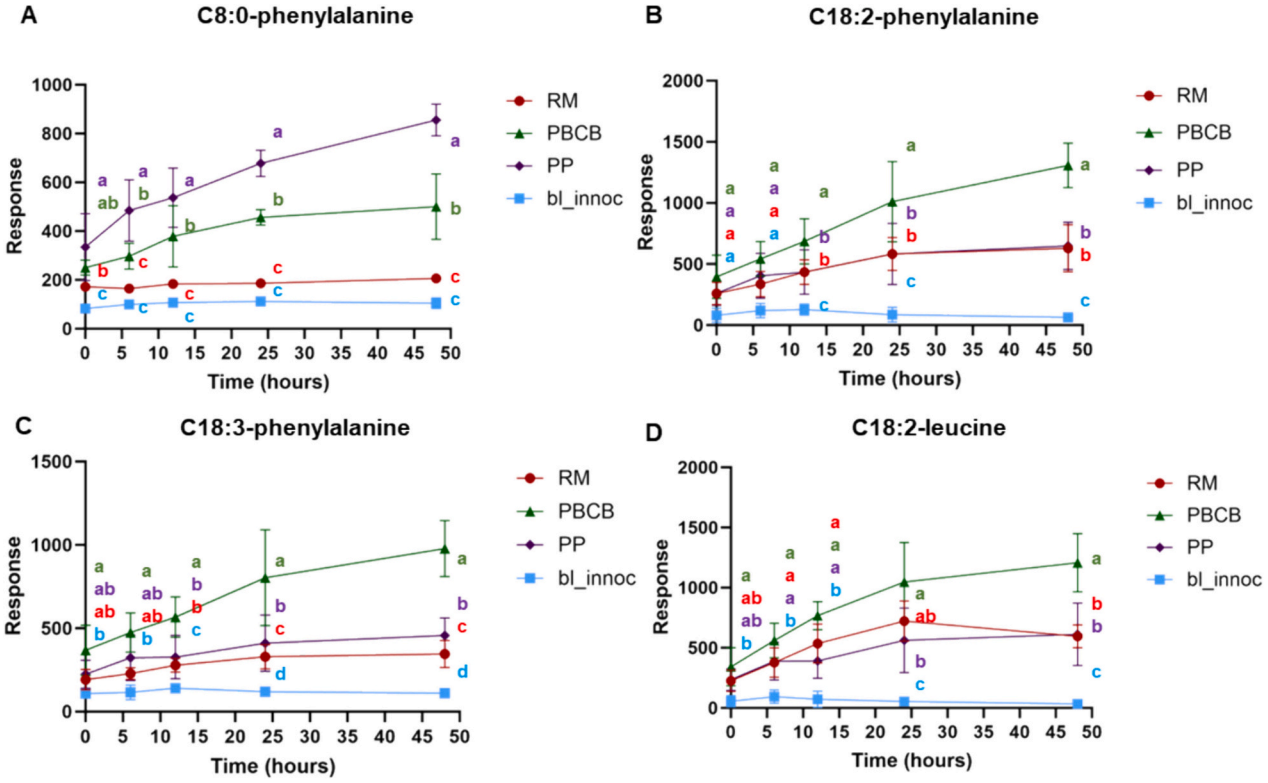

Fig. 4. Response of (A) C8:0-phenylalanine, (B) C18:2-phenylalanine, (C) C18:3-pheynlalanine, (D) C18:2-leucine. Notes: RM beef patty, PBCB plant-based commercial patty, PP plant-based homemade patty, bl_inoculum, sample without any substrate. The different letters indicated the significant difference by two-way ANOVA analysis for different groups at the same time point.

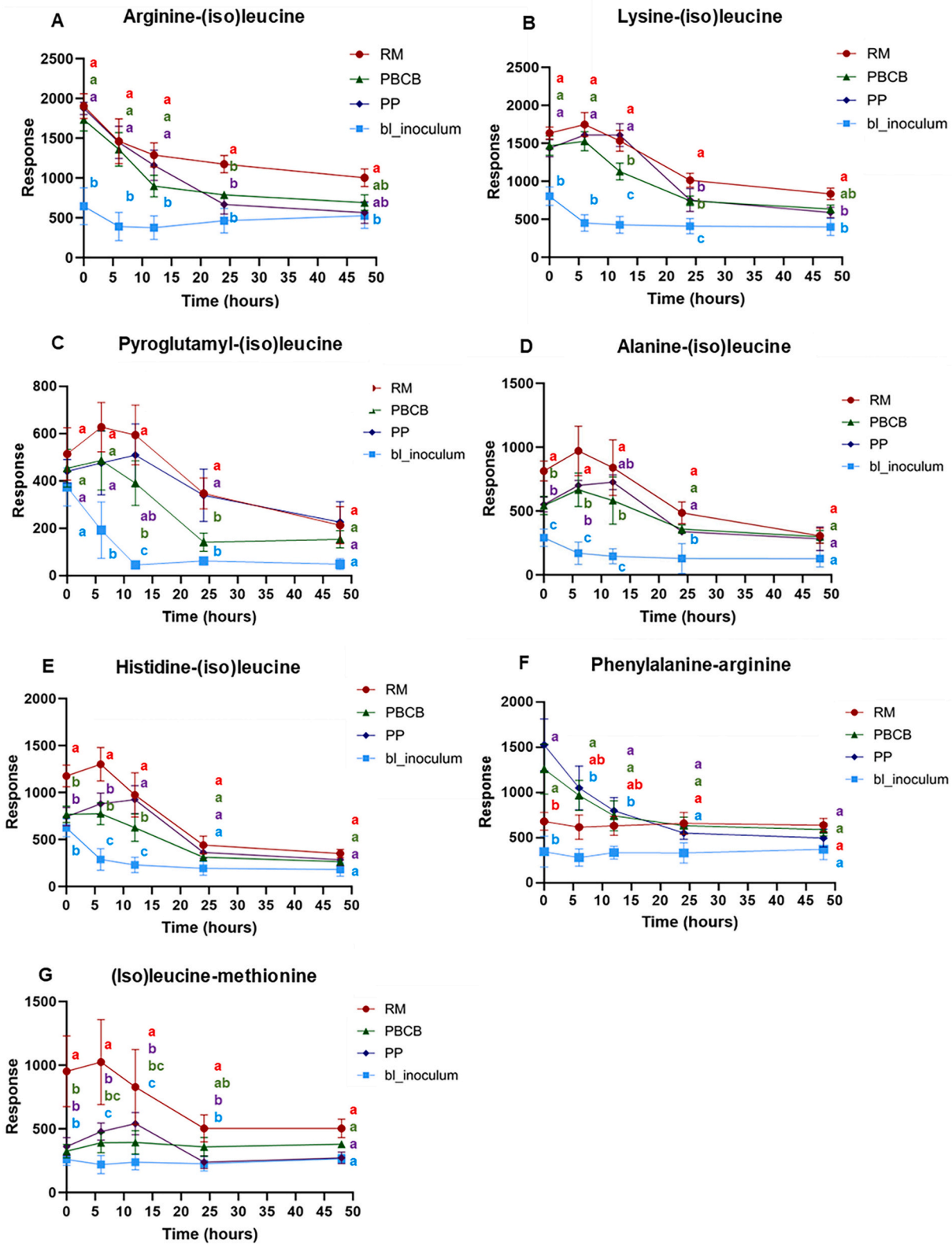

Fig. 5. Response of (A) arginine-(iso)leucine, (B) lysine-(iso)leucine, (C) pyroglutamyl-(iso)leucine, (D) alanine-(iso)leucine, (E) histidine-(iso)leucine, (F) phenylalanine-arginine and (G) (Iso)leucine-methionine. Notes: RM beef patty, PBCB plant-based commercial patty, PP plant-based homemade patty, bl_inoculum, sample without any substrate. The different letters indicated the significant difference by two-way ANOVA analysis for different groups at the same time point.

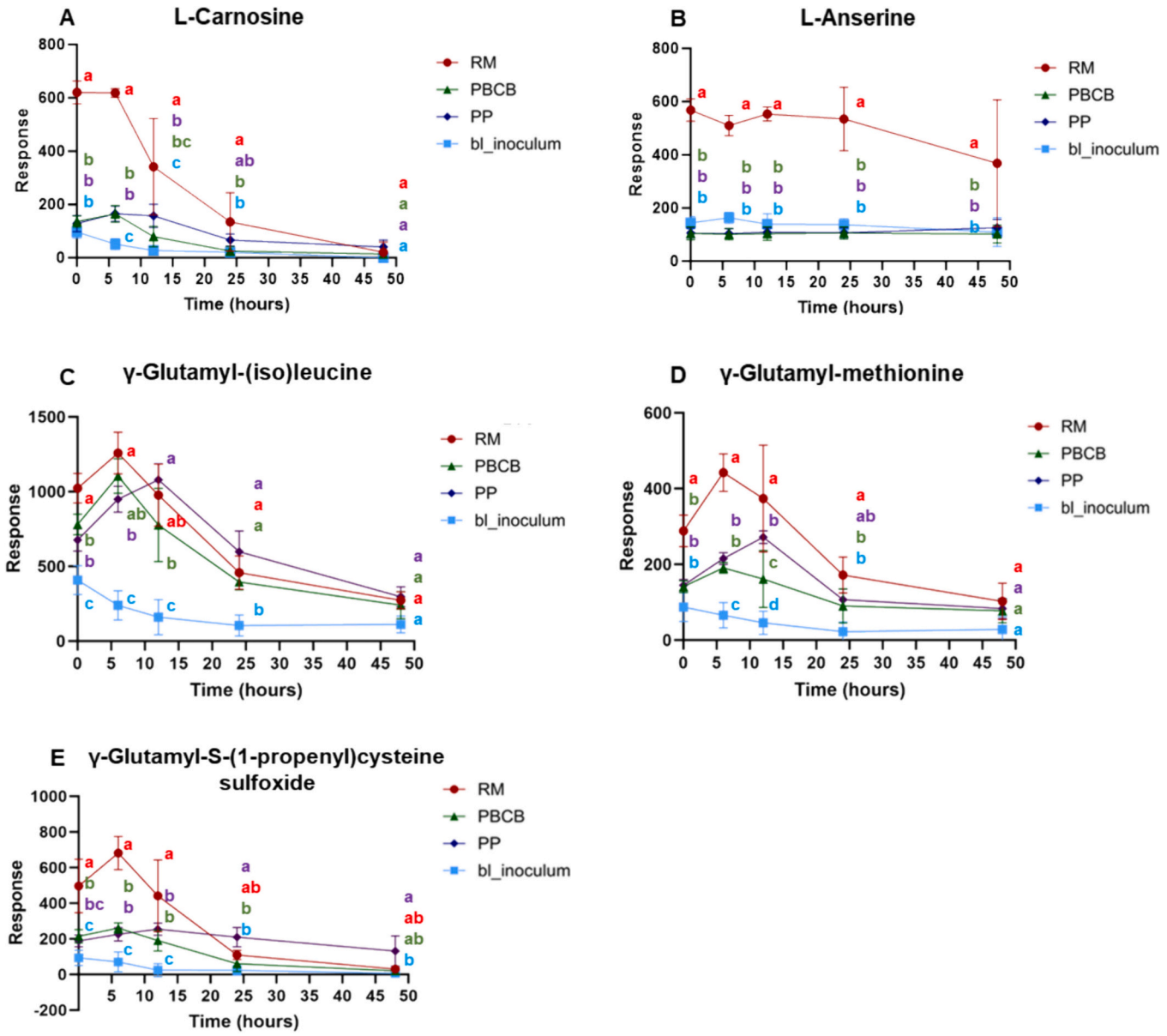

Fig. 6. Response of (A) L-carnosine (B) L-anserine, (C) gamma-glutamyl-(iso)leucine, (D) gamma-glutamyl-methionine, and (E) gamma-glutamyl-S-(1-propenyl) cysteine sulfoxide. Notes: RM beef patty, PBCB plant-based commercial patty, PP plant-based homemade patty, bl_inoculum, sample without any substrate. The different letters indicated the significant difference by two-way ANOVA analysis for different groups at the same time point.

compared to actual meat consumption (Xie et al., 2022). Considering the limitation of *in vitro* digestion models, the current findings demonstrate comparable trends in both matrices regarding the transfer of dipeptides from the small intestine to the colonic stage and their subsequent catabolism by the microbiota.

3.2.2.6. Trends in the metabolism of gamma-glutamyl amino acids. Our study uncovered the ability of the gut microbiota to release specific dipeptides, especially gamma-glutamyl amino acids. Gamma-glutamyl (iso)-leucine (Fig. 6.**C**) was observed to be released during the initial phases of colonic fermentation, followed by its rapid utilization by the microbial communities. While this trend was noticeable across all treatments, it was more apparent in the beef group, as evidenced by the higher basal levels of this compound in the animal-based protein. A similar fluctuating pattern was also observed for gamma-glutamyl methionine and gamma-glutamyl-S-(1-propenyl) cysteine sulfoxide (Fig. 6.**D** and **6.E**, respectively) in the beef meat group, but not in the plant-based analogs. Gamma-glutamyl transpeptidase (GGT) constitutes a group of enzymes that catalyzes the transfer of the gamma-glutamyl group from gamma-glutamyl peptides to other peptides or free amino acids. Studies have implicated GGT in various physiological disorders in mammals, including oxidative stress and gut inflammation (Liu et al., 2023). While these enzymes are primarily present in human biliary epithelial cells, they can also be found in prokaryotic cells (Saini et al., 2021). Our findings indicate that, across all the groups studied, the gut microbiota can return gamma-glutamyl amino acids to baseline levels; however, epithelial cells may absorb these compounds during the early stages of colonic fermentation. Consequently, further research is needed to explore the potential effects of gamma-glutamyl-methionine intake and gamma-glutamyl-S-(1-propenyl) cysteine sulfoxide on intestinal health.

4. Conclusions

Our *in-vitro* investigations provided compelling evidence that the digestion of a pea-based PBMA, compared to a beef patty, induces

alterations in the bioaccessibility and protein fermentation of their associated metabolites. By using an untargeted metabolomics approach, we evaluated the rapidly absorbed metabolite-rich fraction during gastrointestinal digestion, unveiling differences in the composition of small peptides and increased bioavailability of free amino acids in animal-based patties.

Subsequently, the untargeted metabolomics approach on *in vitro* colonic fermentation samples revealed distinct trends in GMMs derived from amino acids and peptides, potentially impacting the intestinal microenvironment. Prominently, utilizing a beef patty as a feeding condition led to the anabolism of metabolites associated with gut inflammation, such as 3-methyl-histidine, a constituent of the histidine pathway, and gamma-glutamyl amino acids. At the time, the use of a beef patty also released metabolites with crucial physiological functions for the gut microbiome, including 4-hydroxyproline, carnosine, and anserine, which were catabolized by the gut microbiota and were absent when pea proteins were employed. Additionally, unique compounds found in meat included acetylcarnitine, whose role in gut health is contentious due to the association of the TMAO biosynthesis pathway with cardiovascular disease. Our finding also unveiled that the gut microbiota releases trimethyllysine, primarily observed when beef patties were used as a feeding condition. However, plant-based alternatives also influenced the production of this precursor in the TMAO biosynthesis pathway. Remarkably, the pea-based commercial patties exhibited a high production of N-acyl amino acids during colonic fermentation compared with beef patties. N-acyl amino acids have been associated with key signaling functions in the intestinal tract. Finally, in both animal and plant-based patties, elevated levels of dipeptides were discovered at the initiation of the colonic fermentations, but they were rapidly catabolized after 24 h. Generally, dipeptide levels were more pronounced in beef patties, although there were exceptions, such as phenylalanine-arginine.

Regarding total SCFAs, both the beef-based and the pea-based commercial patties exhibited a higher concentration of total SCFAs after 12 h, with increased concentrations of isobutyric and isovaleric acid reported for the beef-based patty toward the later stages of fermentation. Similarly, no significant differences in ammonia and total phenol content were observed between beef patty and PBCB during the *in vitro* colonic fermentation. Specifically, samples from the beef-based patty group exhibited notably higher fecal indole content than the plant-derived samples. In addition, a general increasing trend was observed for pH levels across all groups during fermentation, with lower levels noted for plant-derived patties after 48 h of fermentation. It is noteworthy that both pea-based patties presented high divergences in the production of certain GMMs. The homemade patty significantly produced a lower amount of SCFAs and presented lower pH values. In addition, total phenol content, tyrosine, and tryptophan levels were higher compared to commercial patties.

CRediT authorship contribution statement

David Izquierdo-Sandoval: Writing – review & editing, Writing – original draft, Visualization, Methodology, Investigation, Formal analysis, Data curation, Conceptualization. **Xiang Duan:** Writing – review & editing, Writing – original draft, Visualization, Methodology, Investigation, Funding acquisition, Formal analysis, Data curation, Conceptualization. **Christos Fryganas:** Supervision, Methodology. **Tania Portolés:** Writing – review & editing, Writing – original draft, Funding acquisition, Conceptualization. **Juan Vicente Sancho:** Writing – review & editing, Writing – original draft, Supervision, Funding acquisition, Conceptualization. **Josep Rubert:** Writing – review & editing, Writing – original draft, Supervision, Resources, Project administration, Methodology, Investigation, Funding acquisition, Formal analysis, Data curation, Conceptualization.

Declaration of competing interest

The authors declare that they have no known competing financial interests or personal relationships that could have appeared to influence the work reported in this paper.

Data availability

Data will be made available on request.

Acknowledgments

The Food Quality and Design chair group at Wageningen University supported this research using internal funding. The authors would like to thank Dr. Justin van der Hooft for advising on using GNPS. D. Izquierdo-Sandoval acknowledges the Ministry of Science, Innovation and University of Spain for funding his research through the FPU predoctoral program (FPU19/01839) and for the financial support received for his research stay at the Wageningen University & Research. X. Duan acknowledges the Ministry of Science and Technology National Foreign Experts Program (20231047). T. Portolés acknowledges the financial support of the Ramon y Cajal Program from the Ministry of Economy and Competitiveness of Spain (RYC-2017-22525). The Research Institute for Pesticides and Water (IUPA) authors acknowledge the financial support of the Ministry of Science, Innovation and University of Spain (Ref PID2021-127346NB-I00).

Appendix A. Supplementary data

Supplementary data to this article can be found online at https://doi.org/10.1016/j.foodchem.2024.140161.

References

Al-Sawalha, N. A., Alshogran, O. Y., Awawdeh, M. S., & Almomani, B. A. (2019). The effects of L-carnosine on development of metabolic syndrome in rats. *Life Sciences, 237*, Article 116905. https://doi.org/10.1016/j.lfs.2019.116905

Bechthold, A., Boeing, H., Schwedhelm, C., Hoffmann, G., Knüppel, S., Iqbal, K., De Henauw, S., Michels, N., Devleesschauwer, B., Schlesinger, S., & Schwingshackl, L. (2019). Food groups and risk of coronary heart disease, stroke and heart failure: A systematic review and dose-response meta-analysis of prospective studies. *In Critical Reviews in Food Science and Nutrition, 59*(7), 1071–1090. https://doi.org/10.1080/10408398.2017.1392288

Blachier, F., Beaumont, M., Andriamihaja, M., Davila, A. M., Lan, A., Grauso, M., … Tomé, D. (2017). Changes in the luminal environment of the colonic epithelial cells and Physiopathological consequences. *In American Journal of Pathology, 187*(3), 476–486. https://doi.org/10.1016/j.ajpath.2016.11.015

Brodkorb, A., Egger, L., Alminger, M., Alvito, P., Assunção, R., Ballance, S., Bohn, T., Bourlieu-Lacanal, C., Boutrou, R., Carrière, F., Clemente, A., Corredig, M., Dupont, D., Dufour, C., Edwards, C., Golding, M., Karakaya, S., Kirkhus, B., Le Feunteun, S., & Recio, I. (2019). INFOGEST static *in vitro* simulation of gastrointestinal food digestion. *Nature Protocols, 14*(4), 991–1014. https://doi.org/10.1038/s41596-018-0119-1

Cohen, L. J., Esterhazy, D., Kim, S. H., Lemetre, C., Aguilar, R. R., Gordon, E. A., … Brady, S. F. (2017). Commensal bacteria make GPCR ligands that mimic human signalling molecules. *Nature, 549*(7670), 48–53. https://doi.org/10.1038/nature23874

Cuparencu, C., Rinnan, Å., & Dragsted, L. O. (2019). Combined markers to assess meat intake—Human Metabolomic studies of discovery and validation. *Molecular Nutrition & Food Research, 63*(17), 763–772. https://doi.org/10.1002/mnfr.201900106

Davydova, E., Shimazu, T., Schuhmacher, M. K., Jakobsson, M. E., Willemen, H. L. D. M., Liu, T., … Falnes, P. (2021). The methyltransferase METTL9 mediates pervasive 1-methylhistidine modification in mammalian proteomes. *Nature Communications, 12*(1), 891. https://doi.org/10.1038/s41467-020-20670-7

De Marchi, M., Costa, A., Pozza, M., Goi, A., & Manuelian, C. L. (2021). Detailed characterization of plant-based burgers. *Scientific Reports, 11*(1), 2049. https://doi.org/10.1038/s41598-021-81684-9

Deda, O., Gika, H. G., Wilson, I. D., & Theodoridis, G. A. (2015). An overview of fecal sample preparation for global metabolic profiling. *In Journal of Pharmaceutical and Biomedical Analysis, 113*, 137–150. https://doi.org/10.1016/j.jpba.2015.02.006

Folz, J., Culver, R. N., Morales, J. M., Grembi, J., Triadafilopoulos, G., Relman, D. A., … Fiehn, O. (2023). Human metabolome variation along the upper intestinal tract. *Nature Metabolism, 5*(5), 777–788. https://doi.org/10.1038/s42255-023-00777-z

Han, J., Wang, Z., Lu, C., Zhou, J., Li, Y., Ming, T., … Su, X. (2021). The gut microbiota mediates the protective effects of anserine supplementation on hyperuricaemia and

associated renal inflammation. *Food & Function, 12*(19), 9030–9042. https://doi.org/10.1039/d1fo01884a

Huyan, Z., Pellegrini, N., Steegenga, W., & Capuano, E. (2022). Insights into gut microbiota metabolism of dietary lipids: The case of linoleic acid. *Food & Function, 13*, 4513–4526. https://doi.org/10.1039/d1fo04254h

Isenring, J., Bircher, L., Geirnaert, A., & Lacroix, C. (2023). In vitro human gut microbiota fermentation models: Opportunities, challenges, and pitfalls. *Microbiome Research Reports, 2*(1), 2. https://doi.org/10.20517/mrr.2022.15

Israr, M. Z., Bernieh, D., Salzano, A., Cassambai, S., Yazaki, Y., Heaney, L. M., … Suzuki, T. (2021). Association of gut-related metabolites with outcome in acute heart failure. *American Heart Journal, 234*, 71–80. https://doi.org/10.1016/j.ahj.2021.01.006

Koeth, R. A., Lam-Galvez, B. R., Kirsop, J., Wang, Z., Levison, B. S., Gu, X., … Hazen, S. L. (2019). L-carnitine in omnivorous diets induces an atherogenic gut microbial pathway in humans. *Journal of Clinical Investigation, 129*(1), 373–387. https://doi.org/10.1172/JCI94601

Lacalle-Bergeron, L., Izquierdo-Sandoval, D., Sancho, J. V., López, F. J., Hernández, F., & Portolés, T. (2021). Chromatography hyphenated to high resolution mass spectrometry in untargeted metabolomics for investigation of food (bio)markers. *In TrAC - Trends in Analytical Chemistry, 135*, Article 116161. https://doi.org/10.1016/j.trac.2020.116161

Liu, F., Smith, A. D., Wang, T. T. Y., Pham, Q., Yang, H., & Li, R. W. (2023). Multi-omics analysis detected multiple pathways by which pomegranate punicalagin exerts its biological effects in modulating host-microbiota interactions in murine colitis models. *Food & Function, 14*(8), 3824–3837. https://doi.org/10.1039/d3fo00286a

Maas, M. N., Hintzen, J. C. J., Porzberg, M. R. B., & Mecinović, J. (2020). Trimethyllysine: From carnitine biosynthesis to epigenetics. *In International Journal of Molecular Sciences, 21*(24), 1–33. https://doi.org/10.3390/ijms21249451

Moro, J., Tomé, D., Schmidely, P., Demersay, T. C., & Azzout-Marniche, D. (2020). Histidine: A systematic review on metabolism and physiological effects in human and different animal species. *Nutrients, 12*(5), 1414. https://doi.org/10.3390/nu12051414

Nothias, L. F., Petras, D., Schmid, R., Dührkop, K., Rainer, J., Sarvepalli, A., … Dorrestein, P. C. (2020). Feature-based molecular networking in the GNPS analysis environment. *Nature Methods, 17*(9), 905–908. https://doi.org/10.1038/s41592-020-0933-6

Osawa, Y., Mizushige, T., Jinno, S., Sugihara, F., Inoue, N., Tanaka, H., & Kabuyama, Y. (2018). Absorption and metabolism of orally administered collagen hydrolysates evaluated by the vascularly perfused rat intestine and liver in situ. *Biomedical Research (Tokyo), 39*(1), 1–11. https://doi.org/10.2220/biomedres.39.1

Portune, K. J., Beaumont, M., Davila, A. M., Tomé, D., Blachier, F., & Sanz, Y. (2016). Gut microbiota role in dietary protein metabolism and health-related outcomes: The two sides of the coin. *Trends in Food Science and Technology, 57*, 213–232. https://doi.org/10.1016/j.tifs.2016.08.011

Raffner Basson, A., Gomez-Nguyen, A., Lasalla, A., Buttó, L., Kulpins, D., Warner, A., Di Martino, L., Ponzani, G., Osme, A., Rodriguez-Palacios, A., & Cominelli, F. (2021). Replacing animal protein with soy-pea protein in an 'american 'Diet' controls murine Crohn disease-like ileitis regardless of Firmicutes: Bacteroidetes ratio. *Journal of Nutrition, 151*(3), 579–590. https://doi.org/10.1093/jn/nxaa386

Rawla, P., Sunkara, T., & Barsouk, A. (2019). Epidemiology of colorectal cancer: Incidence, mortality, survival, and risk factors. *Przeglad Gastroenterologiczny, 14*(2), 89–103. https://doi.org/10.5114/pg.2018.81072

Ruttkies, C., Schymanski, E. L., Wolf, S., Hollender, J., & Neumann, S. (2016). MetFrag relaunched: Incorporating strategies beyond in silico fragmentation. *Journal of Cheminformatics, 8*(1), 3. https://doi.org/10.1186/s13321-016-0115-9

Saini, M., Kashyap, A., Bindal, S., Saini, K., & Gupta, R. (2021). Bacterial Gamma-Glutamyl Transpeptidase, an Emerging Biocatalyst: Insights Into Structure–Function Relationship and Its Biotechnological Applications. *In Frontiers in Microbiology, 12*. https://doi.org/10.3389/fmicb.2021.641251

Shimizu, M., & Son, D. O. (2007). Food-derived peptides and intestinal functions. *In Current Pharmaceutical Design, 13*, 885–895. https://doi.org/10.2174/138161207780414287

Sri Harsha, P. S. C., Wahab, R. A., Cuparencu, C., Dragsted, L. O., & Brennan, L. (2018). A metabolomics approach to the identification of urinary biomarkers of pea intake. *Nutrients, 10*(12), 1–17. https://doi.org/10.3390/nu10121911

Talavera Andújar, B., Aurich, D., Aho, V. T. E., Singh, R. R., Cheng, T., Zaslavsky, L., … Schymanski, E. L. (2022). Studying the "Parkinson"s disease metabolome and exposome in biological samples through different analytical and cheminformatics approaches: A pilot study. *Analytical and Bioanalytical Chemistry, 414*(25), 7399–7419. https://doi.org/10.1007/s00216-022-04207-z

Toribio-Mateas, M. A., Bester, A., & Klimenko, N. (2021). Impact of plant-based meat alternatives on the gut microbiota of consumers: A real-world study. *Foods, 10*(9), 2040. https://doi.org/10.3390/foods10092040

Tsugawa, H., Cajka, T., Kind, T., Ma, Y., Higgins, B., Ikeda, K., Kanazawa, M., Vandergheynst, J., Fiehn, O., & Arita, M. (2015). MS-DIAL: Data-independent MS/MS deconvolution for comprehensive metabolome analysis. *Nature Methods, 12*(6), 523–526. https://doi.org/10.1038/nmeth.3393

Vanden Bussche, J., Marzorati, M., Laukens, D., & Vanhaecke, L. (2015). Validated high resolution mass spectrometry-based approach for Metabolomic fingerprinting of the human gut phenotype. *Analytical Chemistry, 87*(21), 10927–10934. https://doi.org/10.1021/acs.analchem.5b02688

Waldum, H. L., Hauso, O., & Fossmark, R. (2014). The regulation of gastric acid secretion - clinical perspectives. *In Acta Physiologica, 210*(2), 239–256. https://doi.org/10.1111/apha.12208

Wang, M., Carver, J. J., Phelan, V. V., Sanchez, L. M., Garg, N., Peng, Y., … Bandeira, N. (2016). Sharing and community curation of mass spectrometry data with global natural products social molecular networking. *Nature Biotechnology, 34*(8), 828–837. https://doi.org/10.1038/nbt.3597

Wu, G. (2020). Important roles of dietary taurine, creatine, carnosine, anserine and 4-hydroxyproline in human nutrition and health. *Amino Acids, 52*(3), 329–360. https://doi.org/10.1007/s00726-020-02823-6

Xia, J., Sinelnikov, I. V., & Wishart, D. S. (2011). MetATT: A web-based metabolomics tool for analyzing time-series and two-factor datasets. *Bioinformatics, 27*(17), 2455–2456. https://doi.org/10.1093/bioinformatics/btr392

Xie, Y., Cai, L., Huang, Z., Shan, K., Xu, X., Zhou, G., & Li, C. (2022). Plant-based meat analogues weaken gastrointestinal digestive function and show less digestibility than real meat in mice. *Journal of Agricultural and Food Chemistry, 70*(39), 12442–12455. https://doi.org/10.1021/acs.jafc.2c04246

Xu, H., Pan, L. B., Yu, H., Han, P., Fu, J., Zhang, Z. W., … Wang, Y. (2022). Gut microbiota-derived metabolites in inflammatory diseases based on targeted metabolomics. *Frontiers in Pharmacology, 13*. https://doi.org/10.3389/fphar.2022.919181

Zhou, Z., Amer, H., Sultani, A., Nasr, P., Wang, Y., Corradini, M. G., … Rogers, M. A. (2023). The digestive fate of beef versus plant-based burgers from bolus to stool. *Food Research International, 167*, Article 112688. https://doi.org/10.1016/j.foodres.2023.112688

Zong, X., Fan, Q., Yang, Q., Pan, R., Zhuang, L., Xi, R., Zhang, R., & Tao, R. (2022). Trimethyllysine, a trimethylamine N-oxide precursor, predicts the presence, severity, and prognosis of heart failure. *Frontiers in Cardiovascular Medicine, 9*(September), 1–12. https://doi.org/10.3389/fcvm.2022.907997